Article

Comparative Assessment of Proportions of Urea in Blend for Nitrogen-Rich Pyrolysis: Characteristics and Distribution of Bio-Oil and Biochar

Zhisen He, Shanjian Liu,* Wenjing Zhao, Mengqian Yin, Mei Jiang, and Dongmei Bi

Read Online

ACCESS | 📊 Metrics & More | 📖 Article Recommendations

ABSTRACT: This study aimed to investigate the effect of the urea content on the characteristics and distribution of nitrogen-rich bio-oil and nitrogen-doped biochar. Cellulose, cellobiose, and glucose were used as feedstock. Urea was used as the exogenous nitrogen source in nitrogen-rich pyrolysis at 500 °C. The order of the nitrogen increase in the nitrogen-doped biochar was cellulose < cellobiose < glucose. Nitrogen-doped biochar consisted of abundant nitrogen and nitrogenous functional groups, and the stability of biochar was optimal. The nitrogen-doped biochar obtained from cellulose showed the optimal adsorption performance for diethyl phthalate with 50% urea addition. When the proportion of urea was 20%, the content of anhydro-sugars in bio-oil reached the maximum value (61.86%). Furans and other small-molecule oxygenates were intermediates to produce nitrogenous heterocyclic compounds (NHCs) from cellulose. When the proportion of urea was 40%, the bio-oil had the highest selectivity (91.63%) of NHCs. The NHCs in the obtained bio-oil mainly consisted of pyrroles, pyrimidines, pyridines, imidazoles, and pyrazines. Therefore, the excellent proportion of urea in the blend could promote the generation of high-value NHCs and nitrogen-doped biochar from the nitrogen-rich pyrolysis of cellulose (and its model compounds).
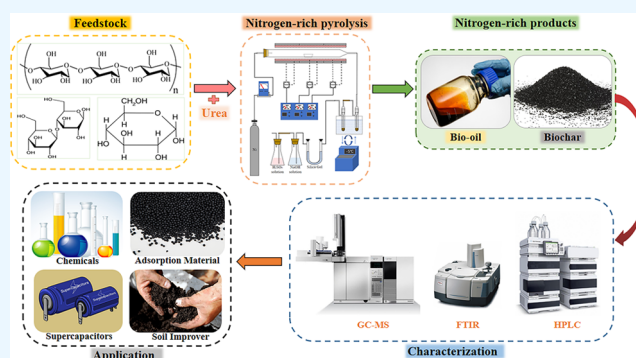
1. INTRODUCTION

Biomass is the only renewable source of carbon, and its application can contribute to the achievement of peak carbon and carbon-neutral strategic goals. Pyrolysis technology has become an important method of high-value biomass utilization because it can efficiently convert biomass into fuels and high-value chemicals.[1] Biochar is a combustible, strongly adsorbed solid-phase product obtained by the pyrolysis of biomass, which can be used in agriculture, energy, and environmental protection.[2] As a liquid-phase product of pyrolysis, bio-oil plays an active and important role in preparing other fine chemicals. When exogenous nitrogen is introduced in the pyrolysis experiment, more valuable bio-oil and biochar are obtained (nitrogen-rich bio-oil and nitrogen-doped biochar). Due to the modifying effect of nitrogen, the CO_2 adsorption and catalytic activities of nitrogen-doped biochar are greatly enhanced compared with biochar. The nitrogen-rich bio-oil is much more valuable due to its richness in nitrogen heterocyclic compounds.[3,4] Li et al.[5] reported the introduction of exogenous nitrogen (ammonium acetate, urea, ammonium sulfate, and ammonium dihydrogen phosphate) in a fixed-bed reactor for the pyrolysis of rice husk, which could convert carbonyl compounds in bio-oil into nitrogen-containing

heterocyclic compounds and improve bio-oil stability. Meanwhile, the resulting nitrogen-doped biochar had high nitrogen content, adsorption activity, specific surface area, and excellent electrochemical properties.

With the development of modern agriculture, phthalates (PAEs) play the role of a participant in agricultural production. Diethyl phthalate (DEP) is a common component of PAEs, which is mainly found in plastics.[6] The large number of PAEs used over the years has resulted in the presence of DEP in soil, water, and even in the air.[7] The treatment and removal of DEP have become the major focus of research by many environmental researchers. However, the high cost of biochemical treatment is a major constraint due to the difficult degradability of DEP. Physical adsorption has been widely used in the remediation of environmental DEP, especially in soil and water environments, mainly by carbon nanotubes,
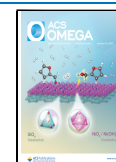
Table 1. Proximate and Elemental Analysis of Cellulose

proximate analysis (wt %, db)			elemental analysis (wt %, daf)			
volatiles	fixed carbon	ash	[C]	[H]	[O][a]	[N]
94.68 ± 0.79	5.29 ± 0.015	0.03 ± 0.004	43.98 ± 0.17	6.13 ± 0.039	49.83 ± 0.21	0.06 ± 0.002

[a]O content was determined by difference (O% = 100% − C% − H% − N%) based on the dry ash-free basis (daf).

activated carbon, and biochar.[8−10] Current research on DEP physical adsorption has focused on the raw material, pyrolysis conditions, DEP adsorption capacity, adsorption concentration, and adsorption time of biochar.[11−14] However, as a DEP or organic pollutant adsorbent, the adsorption stability and desorption rate of the adsorbent should also be considered besides the large specific surface area, hydrophobicity, and adsorption properties. Numerous studies have shown that biochar is an excellent adsorbent for environmental organic pollutants. Chen et al.[15] pyrolyzed bamboo in an ammonia atmosphere. The introduction of NH_3 enriched the resulting bio-oil with nitrogen-containing substances. Meanwhile, the specific surface area, nitrogen content, and nitrogen-containing functional groups of the resulting biochar were significantly increased. Zheng et al.[16] prepared nitrogen-doped carbon with a high specific surface area and good aromatic structure catalyzed by the impregnation of Yunnan pine with an ammonia source. Yin et al.[2] found that the application of nitrogen-doped biochar promoted the conversion of Fe^{3+} into Fe^{2+} in the soil, which was beneficial to the sustainable cultivation of crops.

Considering the significant differences in the thermal decomposition process of different solid nitrogen carriers, it is necessary to study the characteristics of pyrolysis products and related nitrogen migration laws of nitrogen carriers to improve the utilization rate of nitrogen elements. Urea is an inexpensive solid nitrogen carrier with a high nitrogen content and hence can provide exogenous nitrogen for biomass pyrolysis. Cellulose is widely present in industrial and agricultural production waste (e.g., waste paper and bagasse), and therefore it is important to study the relevant pyrolytic properties of cellulose. In this study, cellulose and its modalities (cellobiose and glucose) were used as feedstock and uniformly mixed with urea powder for nitrogen-rich pyrolysis. The nitrogen distribution in the nitrogen-rich pyrolysis chemicals and the effect of different urea mass percentages on the generation of nitrogen-containing groups in nitrogen-doped biochar and nitrogen-rich bio-oil were investigated. Finally, the adsorption performance of the nitrogen-doped biochar prepared by nitrogen-rich pyrolysis on pollutants was investigated using DEP. The findings might have significance for the industrial application of nitrogen-doped biochar, a high value-added product from the nitrogen-rich pyrolysis of biomass.

2. EXPERIMENTAL SECTION

2.1. Experimental Materials. The raw materials for the experiments were cellulose and its molds (cellobiose and glucose), and the nitrogen carrier was urea. The cellulose (≥99%, AR) was produced by Shanghai Aladdin Biochemical Technology Co., Ltd. as a white powder with an average particle size of 25 μm. Cellulose (≥99%, AR) and glucose (≥99%, AR) were produced by Shanghai Yi En Chemical Technology Co. Before pyrolysis, the aforementioned materials were dried in a drying oven at 105 °C for 24 h. The proximate

and elemental analyses of the dried cellulose are shown in Table 1.

The nitrogen-rich pyrolysis reaction system consisted of a carrier gas system, a horizontal tube furnace, a condensing system, and a gas purification unit. The gas purification unit was mainly used for the adsorption of H_2O, HCN, NH_3, and so forth. At 500 °C, nitrogen-rich pyrolysis experiments were performed. In the nitrogen-rich pyrolysis reaction system, N_2 was the carrier gas, the mass flow was 10 mL/min, the pyrolysis holding time was 30 min, and the lowest temperature of the condenser was set to −5 °C.

First, a homogeneous mixture of biomass and nitrogen carrier was loaded into a quartz boat. Then, this quartz boat was placed at the left end of the quartz tube, as shown in Figure 1 (low-temperature zone), and purged with N_2 at a flow
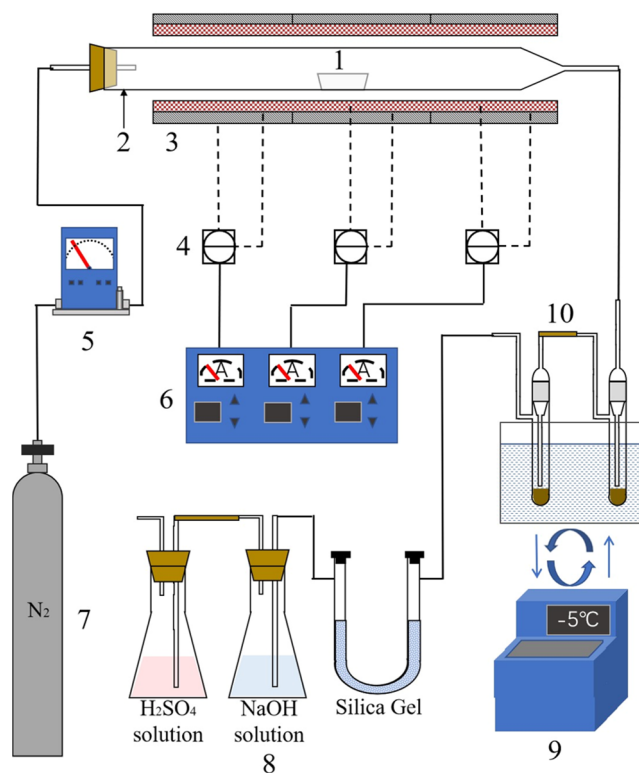

Figure 1. Diagram of nitrogen-rich pyrolysis device: (1) quartz boat; (2) quartz tube; (3) heating furnace; (4) thermocouple for temperature measurement; (5) mass flow meter; (6) temperature controller; (7) nitrogen bottle; (8) gas purification device; (9) circulating water cooling system; and (10) cold trap.

rate of 1000 mL/min for 10 min to remove air. The nitrogen-rich pyrolysis was carried out for 30 min, and the bio-oil was then collected with a cold trap while the biochar was left in the quartz boat. Each experiment was repeated at least three times with a relative error of <5%. The average values are reported in the Results and Discussion section. In addition, the blank experiment of urea pyrolysis was performed to eliminate the

effect of the direct decomposition of urea. The yields of biochar and bio-oil were obtained using eqs 1 and 2.

$$Y_C = \frac{m_C}{m_{urea} + m_{bio}} \qquad (1)$$

$$Y_{bio\text{-}oil} = \frac{m_{bio\text{-}oil}}{m_{urea} + m_{bio}} \qquad (2)$$

Here, Y_C is the yield of pyrolytic biochar, %, m_C is the mass of biochar collected after pyrolysis, m_{bio} is the mass of biomass before pyrolysis, m_{urea} is the mass of added urea, $Y_{bio\text{-}oil}$ is the yield of pyrolytic bio-oil, and $m_{bio\text{-}oil}$ is the mass of bio-oil collected after pyrolysis.

2.2. Biochar Characteristics. *2.2.1. Elemental Analysis (EA).* An elemental analyzer (Vario EL Cube, Elementar, Germany) was used to characterize the elements contained in biochar made by the nitrogen-rich pyrolysis of cellulose and its modalities (cellobiose and glucose). The oxygen content was estimated using the C−H−N−O model and the difference equation. All determination experiments were carried out three times to ensure the reliability of the analytical results, and the standard deviation of the mean values obtained was less than 1%.

2.2.2. Fourier Transform Infrared Spectroscopy (FTIR). The functional groups contained on the surface of biochar obtained by the nitrogen-rich pyrolysis of cellulose and its modalities (cellobiose and glucose) were characterized by FTIR (Nicolet 5700, Thermo Fisher). Prior to testing, the samples were thoroughly mixed with dry potassium bromide at a mass ratio of 1:100. The completely ground mixture was pressed into a thin sheet of ∼13 mm diameter at a pressure of 10 T/cm^2 for 1 min. The resulting sample was then scanned in the spectral range of 4000−400 cm^{-1} with a spectral resolution of 2 cm^{-1}. At the same time, pure KBr pellets of the same thickness of were removed. The obtained spectra were removed from the pure KBr background, which was the infrared spectrum of a single sample.

2.3. Bio-Oil Characteristics. The bio-oil fractions were analyzed using GC-MS (8890N, Agilent Technologies). A capillary column (DB-1701, 60 m × 0.25 mm × 0.25 μm) was used to separate the various compounds in the bio-oil. High-purity helium (≥99%, AR) was maintained as the carrier gas at a flow rate of 1 mL/min. The shunt ratio and injection temperature were set at 60:1 and 280 °C, respectively. The initial temperature of the column chamber was 40 °C, which was then programmed to 240 °C at a ramp rate of 5 °C/min and maintained for 5 min. Approximately 1 μL of bio-oil was injected into each trial using a 7683 series autosampler. The mass spectrometry was performed in the ionization scan mode with an ionization energy of 70 eV and a scan range of 12−550 amu. The ion source temperature was 230 °C, and the interface temperature was 250 °C. The information on the bio-oil components corresponding to the chromatographic peaks was determined based on the NIST17.L database. The relative content of the various compounds in bio-oil was determined from the percentage of the peak area of a single component in the total peak area.

relative content (%)

$$= \frac{\text{relative peak area of single component}}{\text{total relative peak area}} \times 100\% \qquad (3)$$

2.4. DEP Adsorption Experiments. The materials used in the adsorption experiments were as follows. DEP (≥99.5%, AR) purchased from Shanghai Aladdin Co. Ltd., methanol solvent purchased from Tianjin Comio Chemical Reagent Co. Ltd., and phosphate buffer (0.01 mol/L, pH = 7.4). The adsorption experiments were carried out as follows: (1) A DEP stock solution with a concentration of 50 g/L was prepared using methanol as the solvent. (2) A DEP working solution with a concentration of 60 mg/L was prepared, and the stock solution prepared in step (1) was diluted with phosphate buffer to achieve a DEP concentration of 60 mg/L. The phosphate buffer was used as the dilution solution to exclude the effect of pH during the adsorption of DEP on nitrogen-doped biochar. (3) The ratio of nitrogen-doped biochar to DEP working solution was 1:500. Further, 80 mg of nitrogen-doped biochar was weighed and added to the brown sample bottle, and then 40 mL of DEP working solution was added to the brown sample bottle with a pipette gun, and the bottle was sealed. The brown sample bottle was placed in a constant-temperature shaker for 2 days, and 2 mL of the supernatant was taken out after 0, 10, 30, 60, 120, 360, 540, 720, and 1440 min. (4) The DEP concentration of the supernatant was determined by high-performance liquid chromatography (Agilent 1260), and then the amount of DEP adsorbed on the nitrogen-doped biochar was calculated. The working conditions of the liquid chromatograph were as follows: EC-C18 column (4.6 mm × 150 mm × 4 μm), mobile phase of methanol and deionized water mixed at 4:1 by volume, mobile phase flow rate of 1 mL/min, column chamber temperature of 40 °C, injection volume of 10 μL, detection wavelength of 235 nm, and residence time of 2.95 min.

3. RESULTS AND DISCUSSION

3.1. Mass Yields of Pyrolysis Products. Figure 2 shows the yields of bio-oil and biochar from the nitrogen-rich
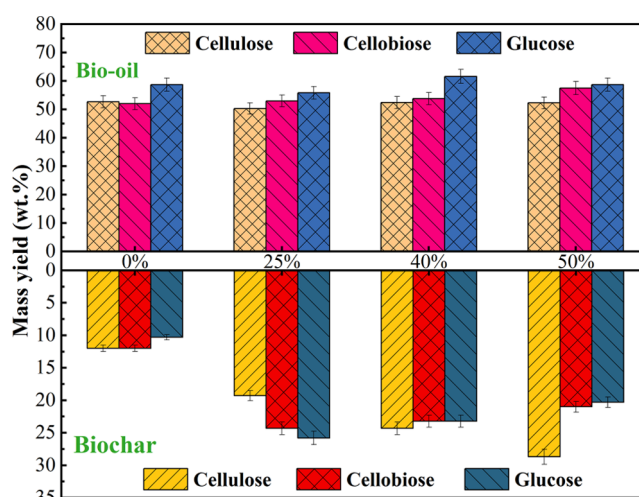

Figure 2. Product yields of cellulose, cellobiose, and glucose with different proportions of urea.

pyrolysis of cellulose and its modalities (cellobiose and glucose). The proportion of urea was 0, 25, 40, and 50%. The yield of bio-oil obtained by nitrogen-rich pyrolysis did not show a significant change. However, the biochar yield from the nitrogen-rich pyrolysis of cellulose tended to increase as the proportion of urea increased from 0 to 50%. The biochar yield

Table 2. Elemental Analysis of Biochar Obtained from Nitrogen-Rich Pyrolysis of Cellulose, Cellobiose, and Glucose

	proportion of urea (wt %)	number	[C]	[H]	[O][a]	[N]
cellulose	0	BC1-0	85.45 ± 1.23	3.35 ± 0.02	11.10 ± 1.25	0
	25	BC1-25	78.41 ± 0.90	3.13 ± 0.03	11.02 ± 1.02	7.43 ± 0.09
	40	BC1-40	75.09 ± 0.86	3.06 ± 0.05	10.85 ± 0.86	11.00 ± 0.12
	50	BC1-50	74.50 ± 0.76	3.02 ± 0.02	10.73 ± 0.95	11.76 ± 0.38
cellobiose	0	BC2-0	86.79 ± 1.56	3.25 ± 0.10	9.96 ± 0.64	0
	25	BC2-25	74.70 ± 0.65	3.13 ± 0.05	8.46 ± 0.43	13.71 ± 1.02
	40	BC2-40	71.44 ± 0.42	3.17 ± 0.06	8.94 ± 0.32	16.45 ± 1.26
	50	BC2-50	70.98 ± 0.32	3.09 ± 0.02	8.55 ± 0.21	17.39 ± 1.58
glucose	0	BC3-0	86.12 ± 2.10	3.35 ± 0.23	10.54 ± 1.06	0
	25	BC3-25	72.84 ± 1.00	3.17 ± 0.32	9.05 ± 0.93	14.94 ± 1.36
	40	BC3-40	70.33 ± 0.59	3.06 ± 0.08	9.37 ± 0.82	17.25 ± 1.85
	50	BC3-50	69.37 ± 0.46	3.02 ± 0.09	9.38 ± 0.71	18.23 ± 2.01

[a]O content was determined by difference (O% = 100% − C% − H% − N%) based on the dry ash-free basis (daf).

from the nitrogen-rich pyrolysis of cellobiose and glucose increased and then decreased with the proportion of urea added and reached the maximum value (24.3 and 25.8%, respectively) when the proportion of urea was 25%.

3.2. Elemental Analysis of Biochar. Table 2 shows the elemental analysis of biochar obtained by nitrogen-rich pyrolysis of cellulose, cellobiose, and glucose. Before and after the addition of urea to cellulose and its modalities (cellobiose and glucose), the content of nitrogen and carbon in the biochar obtained by pyrolysis showed a competitive relationship. As the proportion of urea increased, the content of carbon, hydrogen, and oxygen in the biochar obtained by the nitrogen-rich pyrolysis of the three materials tended to decrease due to the migration of nitrogen into the biochar. When the proportion of urea increased, the nitrogen content in the biochar obtained from the nitrogen-rich pyrolysis of the three materials gradually increased. This indicated that the nitrogen in the urea migrated well into the biochar during nitrogen-rich pyrolysis. The order of the increase in nitrogen in the nitrogen-doped biochar obtained from the three materials was as follows: cellulose < cellobiose < glucose. Therefore, the lower the degree of polymerization of sugars, the more the nitrogen was doped in biochar. The nitrogen-doped biochar obtained from glucose contained the maximum amount of nitrogen, which might be attributed to the large number of carbonyl groups present in glucose as the main nitrogen-doped bonds.[17]

3.3. Chemical Structure of Biochar. The FTIR spectra of nitrogen-doped biochar derived from different materials and the proportion of urea are shown in Figure 3. The main functional groups corresponding to the transmission peaks are listed in Table 3. Figure 3 shows that the trend of the absorption peaks of the biochar derived from cellulose and its modalities (cellobiose and glucose) without the addition of urea was the same. However, as glucose was obtained by the hydrolysis of cellulose or cellobiose, the unsaturated hydrocarbon bonds were partially saturated during the hydrolysis process. Hence, the absorption peak of unsaturated hydrocarbon bonds in glucose was weaker than that in cellulose and cellobiose. The FTIR spectra of biochar derived from different materials and the proportion of urea were similar. When the proportion of urea increased from 0 to 50%, the intensity of the absorption peak of nitrogen-doped biochar located near 3300 cm^{-1} gradually increased. The absorption peak at 3700−3380 cm^{-1} originated from the stretching modes of O−H and N−H bonds of hydroxyl and amino groups.[16] The intensity of
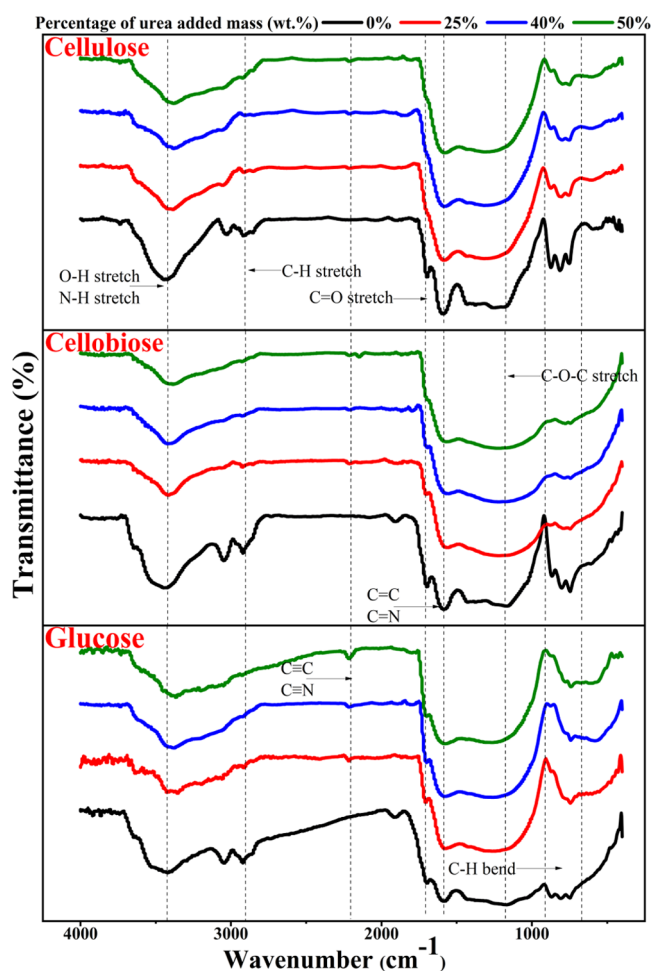

Figure 3. FTIR spectra profiles of biochar obtained by co-pyrolysis of cellulose, cellobiose, glucose and urea.
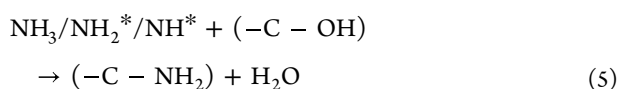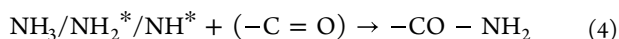
this absorption peak first decreased and then increased as the proportion of urea increased, which stemmed from the introduction of N−H bonds after the addition of urea. The peak at 3000−2700 cm^{-1} was associated with the C−H bond stretching vibration, and its disappearance indicated that the nitrogen replaced the C−H bond on the benzene ring to form the pyridine nitrogen ring.[18,19] When the proportion of urea was 50%, the absorption peak at 2400−2100 cm^{-1} of biochar derived from cellobiose and glucose was associated with the C≡N.[20] The absorption peak located at 1900−1650 cm^{-1}

Table 3. Main Functional Groups Corresponding to FTIR Absorption Peaks of Biochar

wavenumber, cm^{-1}	functional groups	compounds
3700–3380	O–H stretching, N–H stretching	hydroxy, amino[16]
3000–2700	saturated C–H stretching	aliphatic and cycloalkanes[18,19]
2400–2100	C≡C, C≡N	alkynes and nitrile[20]
1900–1650	C=O	aldehyde and aldehyde ketone[21,22]
1675–1500	C=C, C=N	aromatic benzene rings[23]
1300–1000	C–O–C stretching vibration	glycosidic bond, pyran ring ether bond[24,25]
1000–650	unsaturated C–H bending vibration	aldehydes in the form of benzene ring and enol[20]
650–400	C–C stretching vibration	pure graphite or amorphous C–C

corresponded to the C=O stretching vibration, and the disappearance of this peak as the proportion of urea increased indicated that the condensation reaction of amino and carbonyl groups occurred in the nitrogen-doped biochar.[21,22] As the proportion of urea increased, the intensity of the absorption peak corresponding to the aromatic C=C stretching showed an increasing trend. This fact indicated that the addition of urea promoted the condensation reaction of the biochar during pyrolysis, which resulted in the higher aromaticity of biochar. The peak at 1300–1000 cm^{-1} was ascribed to the glycosidic bond and the C–O–C stretching vibration of the pyran ring, which was only present in the biochar obtained by the pyrolysis of the three materials individually.[24–26] This fact indicated that the addition of urea promoted the depolymerization of the glycosidic and pyranic rings.

3.4. Chemical Composition of Bio-Oil. Based on the characteristic functional groups of the chemical components, the organic phases of the bio-oil obtained by the co-pyrolysis of cellulose and urea were classified into seven groups: acids, carbonyl groups (aldehydes and ketones), anhydro-sugars (mainly levoglucan), furans, phenols, and nitrogen-containing compounds. The relative content of all of these groups is shown in Figure 4a. After the addition of urea, the relative content of carbonyl groups and furan compounds decreased significantly. The changes in the carbonyl groups and furan compounds indicated the occurrence of the Maillard reaction and condensation reaction of the amine group and carbonyl group in the pyrolysis process. Furans and other small-molecule oxygenates (ethanol aldehydes, hydroxy acetone, aldehydes, and so on) from cellulose decomposition were the intermediates for the production of nitrogen-containing compounds. After the addition of urea, furans and other small-molecule oxygenates reacted directly with ammonia to form nitrogenous heterocyclic compounds (NHCs). The possible reaction equations of the small-molecule oxygenates with NH$_3$, NH$_2$* and NH* generated by urea are as follows:[27]

$$NH_3/NH_2^*/NH^* + (-C = O) \rightarrow -CO - NH_2 \quad (4)$$

$$NH_3/NH_2^*/NH^* + (-C - OH)$$
$$\rightarrow (-C - NH_2) + H_2O \quad (5)$$

As shown in Figure 4a, the content of anhydro-sugars first increased and then decreased with the increase in the addition
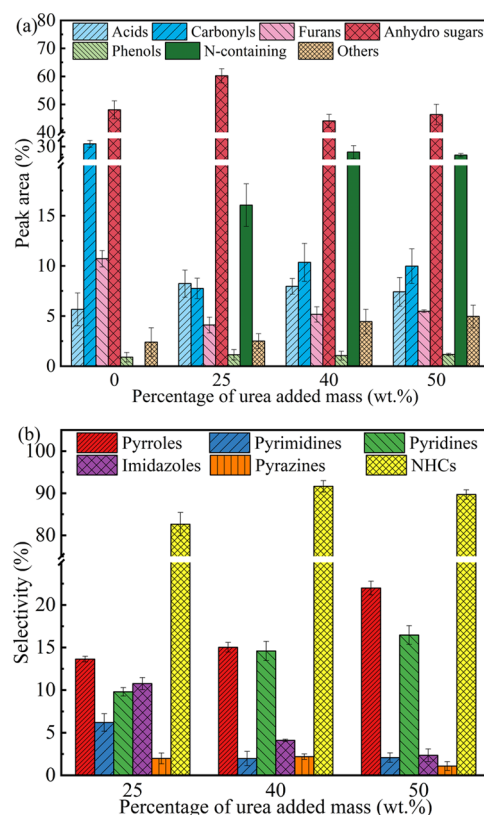

Figure 4. Content of chemical components in bio-oil from nitrogen-rich pyrolysis of cellulose and urea: (a) acids, carbonyls, furans, dehydrated sugars, phenols, and others; (b) nitrogen-containing compounds.

amount of urea and reached the maximum value (61.86%) when the proportion of urea was 20%. This result indicated that the selectivity of anhydro-sugars in the bio-oil could be improved by adding a small amount of urea (the proportion of urea ≤25%). After the introduction of urea, nitrogen-containing compounds were detected in the bio-oil. The content of nitrogen-containing compounds first increased and then decreased with the increase in the addition amount of urea, and reached the maximum value (26.57%) when the proportion of urea was 40%. Nitrogen-containing compounds, especially NHCs (e.g., pyrroles, indoles, pyridines, and their derivatives), are platform compounds for synthesizing agricultural chemicals and drugs.[28,29] As shown in Figure 4b, the selectivity of NHCs among the nitrogen-containing compounds in the bio-oil was high and reached the maximum value (91.63%) when the proportion of urea was 40%. Under these conditions, the maximum percentage of total nitrogen-containing compounds in the bio-oil was achieved. The NHCs in the obtained bio-oil mainly consisted of pyrroles, pyrimidines, pyridines, imidazoles, and pyrazines. The selectivity of pyrimidines, pyrazines, and imidazoles showed a continuous decreasing trend with the increase in the addition amount of urea. However, when the proportion of urea was 50%, pyrroles and pyridines were the main components in the NHCs, and the selectivity of these compunds reached the maximum value (21.99% and 16.47%, respectively).

3.5. Analysis of DEP Adsorption. Different types of biochar were used for DEP adsorption, when the proportion of urea was 50%. The adsorption of DEP at different adsorption times is shown in Figure 5. The adsorption capacity of DEP by
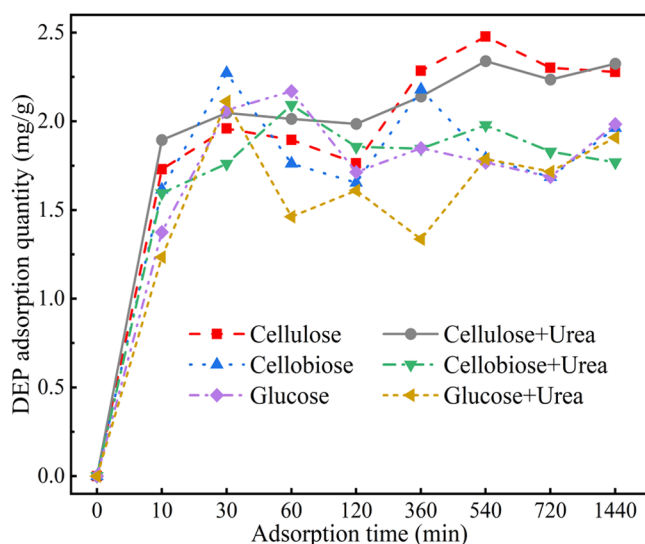
Figure 5. Adsorption of DEP on different types of nitrogen-doped biochar at different adsorption times.

different biochar under different adsorption times was calculated using the following formula:

$$Q_t = \frac{(C_0 - C_t)V}{m} \tag{6}$$

where Q_t represents the amount of DEP adsorbed by different types of biochar at different times, mg/g; C_0 and C_t represent the DEP concentrations in the solution at the initial time and at different times, respectively, mg/L; V represents the volume of the solution, L; and m represents the mass of different types of biochar in the solution, g.

The adsorption of DEP by different types of biochar showed similar conditions. The concentration of DEP in the solution showed a decreasing trend after the adsorption of six different types of biochar for different times, ranging from 55 to 57 mg/L. The adsorption of DEP by biochar was mainly divided into surface adsorption and partitioning. Surface adsorption, as physical adsorption, occurs widely in the adsorption process of biochar to various adsorbates. Partitioning occurs mainly in high-concentration solutions, and the specific adsorption mechanism can be described as a result of the combined effect of pore filling, hydrophobic, and hydrogen bonding.[30] As shown in Figure 5, no significant difference was found in the amount of DEP adsorbed by biochar obtained from cellulose, cellobiose, and glucose. However, the desorption rate of DEP by the biochar obtained from cellulose was lower than that of cellobiose and glucose. In other words, it had better adsorption stability. The order of adsorption performance of non-nitrogen-doped biochar for DEP was as follows: cellulose > cellobiose > glucose. With the addition of urea, the nitrogen-doped biochar obtained by the co-pyrolysis of cellulose and urea showed the optimal performance for DEP adsorption. Meanwhile, the adsorption amount of DEP was higher than that of other biochar after 10 and 1440 min: 1.90 and 2.33 mg/g, respectively. After the addition of urea, the adsorption stability of the biochar obtained from cellulose was better than that without urea. When the adsorption time was not more than 120 min, the adsorption amount of DEP by nitrogen-doped biochar obtained from cellulose was higher than that by non-nitrogen-doped biochar. When the adsorption time was more than 120 min, the adsorption amount of DEP by

nitrogen-doped biochar obtained from cellulose was not significantly different from that by undoped biochar. However, the nitrogen-doped biochar was more stable, suitable for long-lasting adsorption, and less prone to desorption in solution. After adding urea to cellobiose, the resulting nitrogen-doped biochar showed a similar trend to cellulose in terms of DEP adsorption with better adsorption stability, but the amount of DEP adsorbed was lower than that without urea. The adsorption performance of biochar and nitrogen-doped biochar on DEP should not only take into account the surface adsorption of the adsorbate by the physical structure of the biochar itself but also the different chemical sites in the biochar that can affect its adsorption availability.[31] In previous studies, the biochar obtained by co-pyrolysis with urea formed more microporous structures, and abundant nitrogen and new nitrogen-containing functional groups were introduced into the biochar, such as pyridine nitrogen and pyrrole nitrogen.[32] The new functional groups could provide more adsorption sites for chemisorption, which would allow the nitrogen-doped biochar to exhibit better DEP adsorption performance. During the adsorption of DEP, both nitrogen-doped and non-nitrogen-doped biochar had a certain number of pore structures as well as adsorption sites. As the concentration of adsorbate increased, the adsorption capacity of the biochar reached saturation.[30] The addition of urea introduced microporous structures as well as abundant nitrogen elements and nitrogen-containing functional groups into the biochar. More importantly, the ordered aromatic structure was created in the biochar during the formation of a solid product, which increased its aromatization and graphitization and improved the stability of biochar. Therefore, the doping of nitrogen in biochar had a positive effect in terms of improving its adsorption stability to DEP and reducing the desorption rate. In this study, the order of adsorption performance of the six different biochar for DEP was as follows: cellulose with urea > cellulose > cellobiose with urea > cellobiose > glucose > glucose with urea. This might increase the potential for the development and application of nitrogen-doped biochar in the field of adsorption and beyond.

4. CONCLUSIONS

In this study, high value-added nitrogen-containing compounds were prepared in high yields by nitrogen-rich pyrolysis and characterized for their physicochemical properties. The proportion of urea had a significant effect on the yield of nitrogen-doped biochar and the distribution of elements and functional groups on the surface. The proportion of urea positively correlated with the biochar yield of cellulose from nitrogen-rich pyrolysis. The biochar yield from the nitrogen-rich pyrolysis of cellobiose and glucose increased and then decreased with the proportion of urea added and reached the maximum value (24.3 and 25.8%, respectively) when the proportion of urea was 25%. The order of the increase in nitrogen in the nitrogen-doped biochar obtained from the three materials was as follows: cellulose < cellobiose < glucose. Therefore, the lower the degree of polymerization of sugars, the more the nitrogen was doped in biochar. The content of nitrogen-containing compounds in the bio-oil obtained from the nitrogen-rich pyrolysis of cellulose reached the maximum value (26.57%) when the proportion of urea was 40%. Meanwhile, the selectivity of NHCs reached the maximum value, which was 91.63%. With the addition of urea, abundant nitrogen and nitrogenous functional groups were introduced

into biochar. The aromatization and graphitization degree of biochar were high. The optimal pore structure improved the stability of the nitrogen-doped biochar for DEP adsorption. In conclusion, the nitrogen-doped biochar obtained from cellulose feedstock showed optimal physicochemical properties with 50% urea addition.

■ AUTHOR INFORMATION

Corresponding Author

Shanjian Liu − *School of Agricultural Engineering and Food Science, Shandong University of Technology, Zibo 255049, China;* ⊙ orcid.org/0000-0002-8756-9595; Email: liushanjian08@163.com

Authors

Zhisen He − *School of Agricultural Engineering and Food Science, Shandong University of Technology, Zibo 255049, China*

Wenjing Zhao − *School of Agricultural Engineering and Food Science, Shandong University of Technology, Zibo 255049, China*

Mengqian Yin − *School of Agricultural Engineering and Food Science, Shandong University of Technology, Zibo 255049, China*

Mei Jiang − *School of Agricultural Engineering and Food Science, Shandong University of Technology, Zibo 255049, China*

Dongmei Bi − *School of Agricultural Engineering and Food Science, Shandong University of Technology, Zibo 255049, China*

Complete contact information is available at:
https://pubs.acs.org/10.1021/acsomega.2c06643

Notes

The authors declare no competing financial interest.

■ ACKNOWLEDGMENTS

■ REFERENCES

(1) Zhang, S.; Su, Y.; Xu, D.; Zhu, S.; Zhang, H.; Liu, X. Effects of torrefaction and organic-acid leaching pretreatment on the pyrolysis behavior of rice husk. *Energy* 2018, *149*, 804−813.

(2) Yin, X.; Peñuelas, J.; Sardans, J.; Xu, X.; Chen, Y.; Fang, Y.; Wu, L.; Singh, B. P.; Tavakkoli, E.; Wang, W. Effects of nitrogen-enriched biochar on rice growth and yield, iron dynamics, and soil carbon storage and emissions: A tool to improve sustainable rice cultivation. *Environ. Pollut.* 2021, *287*, No. 117565.

(3) Liu, S.; Zhao, A.; He, Z.; Li, Y.; Bi, D.; Gao, X. Effects of temperature and urea concentration on nitrogen-rich pyrolysis: Pyrolysis behavior and product distribution in bio-oil. *Energy* 2022, *239*, No. 122443.

(4) Zhao, A.; Liu, S.; Yao, J.; Huang, F.; He, Z.; Liu, J. Characteristics of bio-oil and biochar from cotton stalk pyrolysis: Effects of torrefaction temperature and duration in an ammonia environment. *Bioresour. Technol.* 2022, *343*, No. 126145.

(5) Li, K.; Zhu, C.; Zhang, L.; Zhu, X. Study on pyrolysis characteristics of lignocellulosic biomass impregnated with ammonia source. *Bioresour. Technol.* 2016, *209*, 142−147.

(6) Fan, X.; Wang, X.; Zhao, B.; Wan, J.; Tang, J.; Guo, X. Sorption mechanisms of diethyl phthalate by nutshell biochar derived at different pyrolysis temperature. *J. Environ. Chem. Eng.* 2022, *10*, No. 107328.

(7) Yang, Z.; Chen, H.; Wang, J.; Yuan, R.; Wang, F.; Zhou, B. Efficient degradation of diisobutyl phthalate in aqueous solution through electro-Fenton process with sacrificial anode. *J. Environ. Chem. Eng.* 2020, *8*, No. 104057.

(8) Ji, H.; Wang, T.; Huang, T.; Lai, B.; Liu, W. Adsorptive removal of ciprofloxacin with different dissociated species onto titanate nanotubes. *J. Cleaner Prod.* 2021, *278*, No. 123924.

(9) Ji, H.; Xie, W.; Liu, W.; Liu, X.; Zhao, D. Sorption of dispersed petroleum hydrocarbons by activated charcoals: Effects of oil dispersants. *Environ. Pollut.* 2020, *256*, No. 113416.

(10) Pirsaheb, M.; Moradi, S.; Shahlaei, M.; Wang, X.; Farhadian, N. A new composite of nano zero-valent iron encapsulated in carbon dots for oxidative removal of bio-refractory antibiotics from water. *J. Cleaner Prod.* 2019, *209*, 1523−1532.

(11) Chen, B.; Zhou, D.; Zhu, L. Transitional adsorption and partition of nonpolar and polar aromatic contaminants by biochars of pine needles with different pyrolytic temperatures. *Environ. Sci. Technol.* 2008, *42*, 5137−5143.

(12) Lattao, C.; Cao, X.; Mao, J.; Schmidt-Rohr, K.; Pignatello, J. J. Influence of molecular structure and adsorbent properties on sorption of organic compounds to a temperature series of wood chars. *Environ. Sci. Technol.* 2014, *48*, 4790−4798.

(13) Wu, Y.; Si, Y.; Zhou, D.; Gao, J. Adsorption of diethyl phthalate ester to clay minerals. *Chemosphere* 2015, *119*, 690−696.

(14) Zhang, H.; Voroney, R. P.; Price, G. W. Effects of temperature and processing conditions on biochar chemical properties and their influence on soil C and N transformations. *Soil Biol. Biochem.* 2015, *83*, 19−28.

(15) Chen, W.; Yang, H.; Chen, Y.; Chen, X.; Fang, Y.; Chen, H. Biomass pyrolysis for nitrogen-containing liquid chemicals and nitrogen-doped carbon materials. *J. Anal. Appl. Pyrolysis* 2016, *120*, 186−193.

(16) Zheng, Y.; Wang, Z.; Liu, C.; Tao, L.; Huang, Y.; Zheng, Z. Integrated production of aromatic amines, aromatic hydrocarbon and N-heterocyclic bio-char from catalytic pyrolysis of biomass impregnated with ammonia sources over Zn/HZSM-5 catalyst. *J. Energy Inst.* 2020, *93*, 210−223.

(17) Xie, C.; Song, J.; Hua, M.; Hu, Y.; Huang, X.; Wu, H.; Yang, G.; Han, B. Ambient-temperature synthesis of primary amines via reductive amination of carbonyl compounds. *ACS Catal.* 2020, *10*, 7763−7772.

(18) Kanwal, S.; Chaudhry, N.; Munir, S.; Sana, H. Effect of torrefaction conditions on the physicochemical characterization of agricultural waste (sugarcane bagasse). *Waste Manage.* 2019, *88*, 280−290.

(19) Yu, J.; Sun, L.; Berrueco, C.; Fidalgo, B.; Paterson, N.; Millan, M. Influence of temperature and particle size on structural characteristics of chars from Beechwood pyrolysis. *J. Anal. Appl. Pyrolysis* 2018, *130*, 127−134.

(20) Cao, J.-P.; Li, L.-Y.; Morishita, K.; Xiao, X.-B.; Zhao, X.-Y.; Wei, X.-Y.; Takarada, T. Nitrogen transformations during fast pyrolysis of sewage sludge. *Fuel* 2013, *104*, 1−6.

(21) Hu, J.; Song, Y.; Liu, J.; Evrendilek, F.; Buyukada, M.; Yan, Y.; Li, L. Combustions of torrefaction-pretreated bamboo forest residues: Physicochemical properties, evolved gases, and kinetic mechanisms. *Bioresour. Technol.* 2020, *304*, No. 122960.

(22) Wang, D.; Liu, L.; Yuan, Y.; Yang, H.; Zhou, Y.; Duan, R. Design and key heating power parameters of a newly-developed household biomass briquette heating boiler. *Renewable Energy* 2020, *147*, 1371−1379.

(23) Sun, H.; Feng, D.; Sun, S.; Zhao, Y.; Zhang, L.; Chang, G.; Guo, Q.; Wu, J.; Qin, Y. Thermal evolution of gas-liquid-solid

products and migration regulation of C/H/O elements during biomass pyrolysis. *J. Anal. Appl. Pyrolysis* **2021**, *156*, No. 105128.

(24) Adeniyi, A. G.; Ighalo, J. O.; Onifade, D. V. Production of biochar from plantain (Musa paradisiaca) fibers using an updraft biomass gasifier with retort heating. *Combust. Sci. Technol.* **2021**, *193*, 60−74.

(25) Tian, X.; Dai, L.; Wang, Y.; Zeng, Z.; Zhang, S.; Jiang, L.; Yang, X.; Yue, L.; Liu, Y.; Ruan, R. Influence of torrefaction pretreatment on corncobs: A study on fundamental characteristics, thermal behavior, and kinetic. *Bioresour. Technol.* **2020**, *297*, No. 122490.

(26) Yin, Y.; Yin, J.; Zhang, W.; Tian, H.; Hu, Z.; Ruan, M.; Song, Z.; Liu, L. Effect of char structure evolution during pyrolysis on combustion characteristics and kinetics of waste biomass. *J. Energy Res. Technol.* **2018**, *140*, No. 072203.

(27) Xu, L.; Yao, Q.; Deng, J.; Han, Z.; Zhang, Y.; Fu, Y.; Huber, G. W.; Guo, Q. Renewable N-heterocycles production by thermocatalytic conversion and ammonization of biomass over ZSM-5. *ACS Sustainable Chem. Eng.* **2015**, *3*, 2890−2899.

(28) Cui, X.-F.; Hu, F.-P.; Zhou, X.-Q.; Zhan, Z.-Z.; Huang, G.-S. Ruthenium-Catalyzed Synthesis of Pyrrolo [1, 2-a] quinoxaline Derivatives from 1-(2-Aminophenyl) pyrroles and Sulfoxonium Ylides. *Synlett* **2020**, *31*, 1205−1210.

(29) Xu, J.; Tan, H.-B.; Zhang, Y.-J.; Tang, D.-Y.; Zhan, F.; Li, H.-y.; Chen, Z.-Z.; Xu, Z.-G. catalyst-free one-pot Synthesis of Densely Substituted pyrazole-pyrazines as Anti-colorectal cancer Agents. *Sci. Rep.* **2020**, *10*, No. 9281.

(30) Guo, R.; Yan, L.; Rao, P.; Wang, R.; Guo, X. Nitrogen and sulfur co-doped biochar derived from peanut shell with enhanced adsorption capacity for diethyl phthalate. *Environ. Pollut.* **2020**, *258*, No. 113674.

(31) Xu, X.; Zheng, Y.; Gao, B.; Cao, X. N-doped biochar synthesized by a facile ball-milling method for enhanced sorption of CO_2 and reactive red. *Chem. Eng. J.* **2019**, *368*, 564−572.

(32) Jiang, M.; Bi, D.; Wang, T.; Gao, Z.; Liu, J. Co-pyrolysis of cellulose and urea blend: Nitrogen conversion and effects of parameters on nitrogenous compounds distributions in bio-oil. *J. Anal. Appl. Pyrolysis* **2021**, *157*, No. 105177.